HCCI Engine Mean Value Model and Control

Xiao Li, Sunbochen Tang

1 Introduction

HCCI (Homogenous Charge Compression Ignition) engine is a novel engine variation. Unlike traditional spark ignition engine, the ignition control of HCCI engine is realized by regulating its charge composition and thermal variables. Developing a high-fidelity model for HCCI engine is crucial for understanding the physical system, however, such model is also difficult due to the complexity of its states. In fact, a low-order model capturing only essential dynamics would be more effective for control design. In this report, we present our effort in reproducing a mean value model found in literature, and rederive and discuss the controller design with stability issues of HCCI engine based on such model. The sources we followed in the literature are three papers closely related to this topic. Paper [1] introduces and derives the mean value model. Paper [2] simplifies the model in the previous paper with a focus on the temperature dynamics and discusses a nonlinear observer based feedback design along with proof of local stability and robustness analysis. Paper [3] uses the same model and analyzes the influence of heat transfer in the system stability, specifically in the case with high dilution.

2 Control problem

Shown in Fig. 1, the engine model used in [1] is a single cylinder engine operating under fixed engine speed N (1000 rpm), constant fuel flow W_f and isothermal intake manifold (363K) condition. The engine model is equipped with external EGR (model in [2] neglects external EGR) and rebreathing lift which are actuated by EGR valve position u_{egr} and exhaust valve rebreathing lift u_{rbl} respectively. Meanwhile, the output $AFR_{exhaust}$ of exhaust and $CA50$ is used to evaluate the combustion performance.

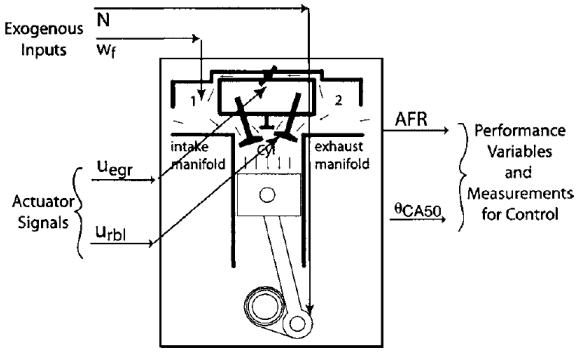

Figure 1. Input and Output of Engine Signals.[1]

Since the combustion is auto-ignited, the key ideal in HCCI engine is about controlling its combustion shape which can be regulated by variables (temperature, pressure and burned gas fraction) in intake charge. In this report, we define the control problem following Paper [2], which uses u_{rbl} to regulate the combustion timing θ_{CA50} by stabilizing the temperature dynamics during fuel step changes.

3 Control-oriented Modeling

Engine component	Manifold filling dynamics	Combustion
Homogenous charge compression ignition engine (Ignore exhaust and intake value lifting dynamics).	Standard modeling using orifice equation, ideal gas law, conservation of mass. Charge mixture of rebreathing during intake stroke and external EGR. Average cylinder flow based on engine cycle.	Five combustion phases (six discrete points) characterized by algebraic equations.

Table 1. HCCI Engine Model.

* Complete state equations, delay equations and algebraic equations for combustion are included in Appendix A.
Simulink Block diagram in Appendix B.
MATLAB code in Appendix C.

In our project, we studied two HCCI engine model and a summary is listed in Table. 1. The first one in [1] is a Mean Value Model with both external EGR and rebreathing lift. Based on the first one, the second one in [2] is a simplified model which removes state variables related to burned gas and external EGR. Both [1] and [2] ignore the intake and exhaust value lifting dynamic in the model and implement a cycle average cylinder flow during intake and exhaust stroke to simplify the dynamics.

3.1 Mean Value HCCI Engine Model*

3.1.1 Manifold Filling Dynamic (MFD)

To characterize the intake charge, paper [1] defines five continues states in MFD which are the manifold mass m_i, burned gas fraction b_i and pressure p_i (Subscript i: 1, 2, *c* and *er* for intake, exhaust manifold, cylinder and exhaust runner respectively and W_{xy} is the flow from x to y). Five states differential equations are based on mass conservation and ideal gas law.

Intake Manifold

$$\frac{d}{dt}m_1 = W_{01} + W_{21} - W_{1c} \quad (1)$$

$$\frac{d}{dt}b_1 = \frac{-W_{01}b_1 + W_{21}(b_2 - b_1)}{m_1} \quad (2)$$

Exhaust Manifold

$$\frac{d}{dt}m_2 = W_{c2} - W_{20} - W_{21} - W_{2c} \quad (3)$$

$$\frac{d}{dt}b_2 = \frac{W_{c2}(b_{er} - b_2)}{m_1} \quad (4)$$

$$\frac{d}{dt}p_2 = \frac{\gamma R}{V_2}\left(W_{c2}\widetilde{T_{er}} - (W_{20} + W_{21} + W_{2c})T_2\right) \quad (5)$$

3.1.2 Combustion

To simplify the intake and exhaust stroke, the cylinder flow is cycle-to-cycle averaged by $W_{1c} = \frac{(1-x_r)}{\tau}m_c$ and $W_{2c} = \frac{x_r}{\tau}m_c$ where m_c is the trapped cylinder mass at intake valve close (IVC), x_r is the mass fraction of internal residual gases at IVC and τ is the engine cycle.

The combustion model covers the combustion stroke as well as the condition (temperature and pressure) at the exhaust stroke. Shown in Fig. 2, the combustion model is basically an algebraic equation system which generates six feature points to characterize the combustion curve. Given the initial condition at IVC, the combustion model can process the data for the remaining five phases including the performance variable CA50 and temperature along with pressure at the exhaust stroke.

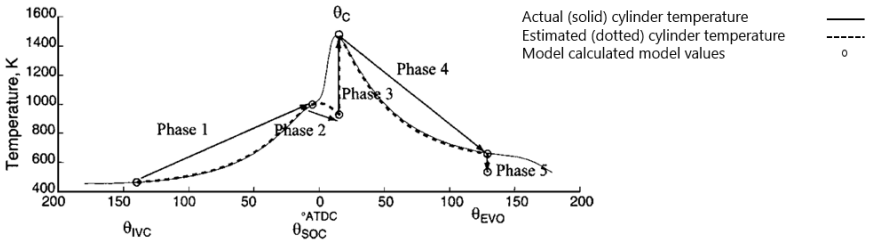

Figure 2. Combustion Model Validation from Literature.[1]

For phase one from IVC to start of combustion (SOC), paper [1] assume it is a polytropic compression process. By Arrhenius integral

$$AR(\theta) = \int_{\theta_{ivc}}^{\theta_{soc}} RR(\vartheta)d\vartheta = 1,$$

we could predict the SOC crank angle position. For phase two from the SOC to the end of combustion (EOC), we are able to predict the combustion duration $\Delta\theta$ as the crank angle degrees between 1% and 90% fuel burned. We assume the heat release only occur instantaneously at the end of combustion which

* Complete state equations, delay equations and algebraic equations for combustion are included in Appendix A.
Simulink Block diagram in Appendix B.
MATLAB code in Appendix C.

produces the third phase. And the fourth expansion phase and fifth blowdown phase are assumed to be polytropic expansion and adiabatic expansion process. By empirical equations determined by experiments and gas law for polytropic process, we can get data points for the remaining fourth and fifth phases. All the equations are listed in Appendix. A. We have successfully reproduced the combustion model and the results is shown in Fig. 3.

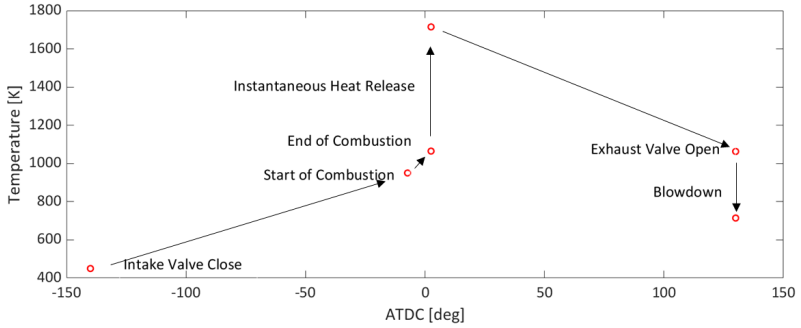

Figure 3. Combustion Model Validation (Code attached in Appendix).

3.1.3 Engine Cycle Delay

To integrate the MFD with the cycle-to-cycle averaged cylinder flow for a complete engine cycle, paper [1] introduces three delay state variables in (6 - 8) to characterize the cycle feature at IVC and exhaust blowdown.

$$W_{c2}(t+\tau) = W_{1c}(t) + W_f(t) + W_{2c}(t) \tag{6}$$

$$T_{er}(t+\tau) = T_{bd}(t) \tag{7}$$

$$b_{er}(t+\tau) = b_{bd}(t) \tag{8}$$

T_{bd} and b_{bd} are the temperature and burned gas fraction, respectively, of the blowdown gas into the exhaust runner which are calculated at phase 5 in the combustion model. T_{bd} and b_{bd} at exhaust value open (EVO) of current engine cycle will be feedback to MFD as T_{er} and b_{er} to calculate b_2 and p_2 in (4-5) at next engine cycle. And (6) is based on mass conservation before and after engine power cycle.

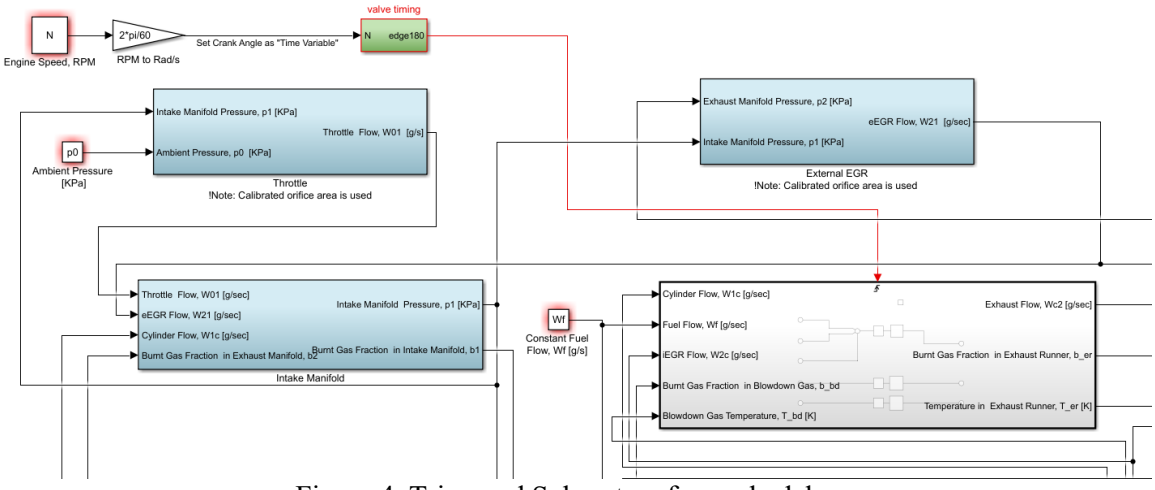

Figure 4. Triggered Subsystem for cycle delay.

To implement the delay states in Simulink, we first tried triggered subsystem. For the first cycle, the delay states uses the initial condition. The trigger event is based on the crank timing. At each IVC, the delay system will update its three delayed state variables and prepare for the combustion model call for the next cycle. However, since our combustion model is an algebraic block, it's hard to integrate it with the continuous MFD within a single Simulink model. The Simulink Model failed to run.

* Complete state equations, delay equations and algebraic equations for combustion are included in Appendix A.
Simulink Block diagram in Appendix B.
MATLAB code in Appendix C.

In that case, we decided to separate the combustion model and delay dynamics with the MFD. Shown in Fig. 5, we only leave MFD and the algebraic block which is used to calculate the condition at IVC in Simulink. Meanwhile, we separate the combustion model out as a MATLAB function. We wrote a MATLAB script to handle the engine cycle delay and pass the state, input and output variable for the entire model (.m file attached in the appendix along with the block diagram).

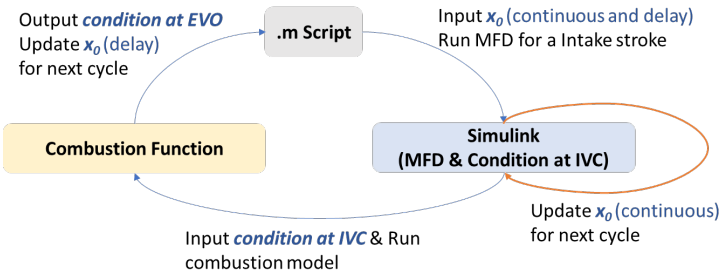

Figure 5. System functional division for engine cycle.

We first assign a meaningful initial condition to the state variables and call the MFD to run through the intake stroke. We update the initial value of continuous state variables for next cycle by their values at the end of the simulation. We then can get the output of the simulation which is the condition at IVC and pass it to the combustion function. At the end of the combustion, we can use the output to update the delay state variables for next cycle.
However, with five continuous and three delay state variables. We just cannot get the initialization right and fail to get temperature values which physically make sense. Unlike SI engine, HCCI engine is sensitive to the charge temperature and pressure condition. Ill conditioned charge at IVC will result in unhealth combustion timing, which subsequently produces ill conditions at IVC for the next cycle. In short, an infeasible initial condition cannot be automatically stabilized in HCCI engine and will lead to unbounded behaviors.

3.2 Simplified HCCI Engine Model*

To mitigate the problem brought by initialization, we decided to adopt a simplified model presented in [2]. Paper [2] removes the dynamics of external EGR and reformulates the state equations without burned gas fractions. Therefore, we are able to bring down numbers of continuous state variables from 5 to 3. (Detail MFD and state equation is attached in Appendix A).

We rebuild the Simulink block and combustion model in [2] and use the same logic in Fig. 5 to complete a simplified HCCI engine model (MATLAB code and block diagram are attached in Appendix B and C). Shown in Fig. 6, we have manifold dynamics responses during a single intake stroke for state variables (m and p) and cylinder flow. For both intake and exhaust manifold, we initialize our MFD using ambient pressure and temperature of isothermal intake manifold. In Fig. 3, we can see that the variables are varying within a reasonable range in terms of their magnitude. However, trends of some curves do not make much sense in physics. For an instance, during the intake stroke, the charge mass in cylinder m_c is decreasing. Therefore, we think the block diagram should reflect MFD, and it is the initial condition which causes the incorrect trend.

* Complete state equations, delay equations and algebraic equations for combustion are included in Appendix A.
Simulink Block diagram in Appendix B.
MATLAB code in Appendix C.

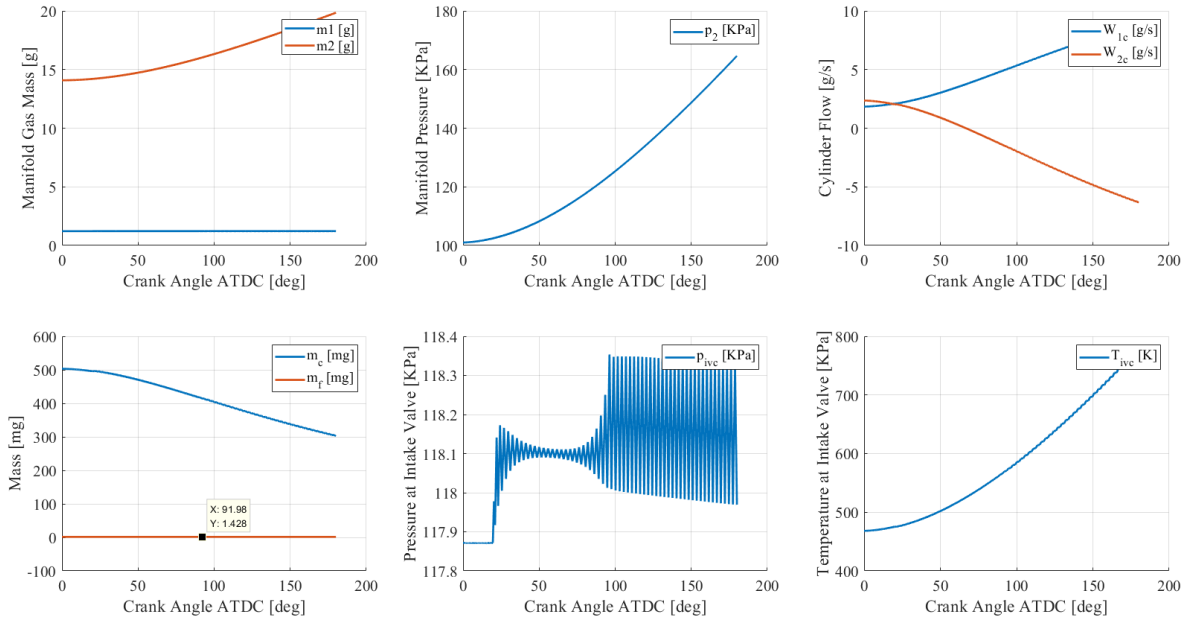

Figure 6. Model validation results for MFD (single cycle).

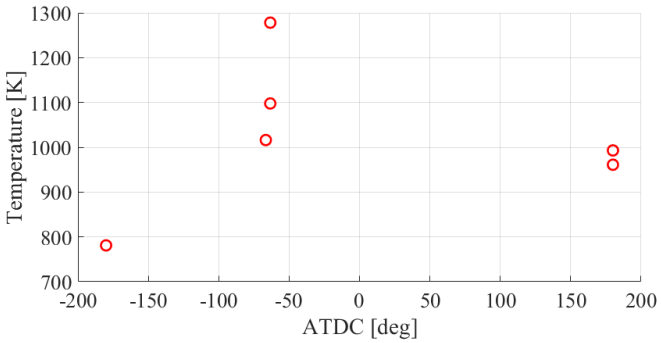

Figure 7. Model validation results for Combustion after MFD (single cycle)

After the MFD, we call the combustion model to run and update a temperature phase graph as Fig. 3. Illustrated in Fig. 7, although the trend looks like correct, the combustion starts much earlier before TDC and the combustion duration is extremely short. Therefore, the engine's power stroke ends far before TDC which will loss significantly amount of power and might not start the engine. The early start of combustion is most likely to be caused by the unreasonably high charge temperature acquired from MFD output. The general trend, again, suggests our combustion model might be correct. It is the initial condition that causes the unhealthy combustion timing observed. Afterwards, when we try further iteration of engine cycles, the state variables as well as the MFD outputs go off the normal magnitude, which matches the unbounded behaviors of HCCI engines with incorrect combustion timing, as mentioned above.

4 Control design

In this section, we describe the nonlinear observer-based control strategy developed in Chiang's work [2]. As discussed in [3], controlled HCCI engine's auto-ignition requires regulation of the charge properties at the intake valve closing (IVC). Specifically, the chosen control strategy aims to develop a nonlinear feedback controller to regulate the combustion timing by stabilizing the temperature at IVC during step changes in fuel injection rates.

* Complete state equations, delay equations and algebraic equations for combustion are included in Appendix A. Simulink Block diagram in Appendix B.
MATLAB code in Appendix C.

4.1 Nonlinear Feedback Controller Design

For controller design purpose, we further simplify the model developed in Section 3. From equations in the full-order model (detailed in [2]), we can rewrite the state equation for T_{ivc} as (9). And we introduce an integral state q to asymptotic regulation of θ_{CA50} set-point in (10).

$$T_{ivc}(k+1) = \left[0.9 f_c\left(T_{ivc}(k), m_f(k)\right) - T_1\right] x_r(k+1) + T_1 \quad (9)$$

$$q(k+1) = q(k) + \tau(\theta_{CA50}^{des} - \theta_{CA50}(k)) \quad (10)$$

Around the desired operating point $\theta_{CA50} = 5°$, θ_{CA50} is approximated as a function of T_{ivc} and m_f, $\tilde{\theta}_{CA50}$ as in (11). Therefore, we acquire a time-invariant nonlinear control system with two states $q(k)$ and $T_{ivc}(k)$, one input $x_r(k)$, and disturbance $m_f(k)$.

$$\tilde{\theta}_{CA50} = g_0(m_f) + g_1(m_f) T_{ivc} \quad (11)$$

The nonlinear feedback controller is designed based on a positive semi-definite Lyapunov function in a discrete system, which reduces the complexity of candidate Lyapunov functions by relaxing the positive definite requirement to positive semidefinite [4]. $V_L(k)$, the chosen Lyapunov function with gain K_I and control law with gain c_L are summarized in (12) and (13).

$$V_L(k) = V^2(k) = \left(K_I q(k) + T_{ivc}(k)\right)^2 \quad (12)$$

$$x_r(k+1) = \left[-K_I\tau\left(\theta_{CA50}^{des} - \tilde{\theta}_{CA50}\left(m_f(k), T_{ivc}(k)\right)\right) - c_L V(k) + T_{ivc}(k) - T_1\right] / \left[0.9 f_c\left(T_{ivc}(k), m_f(k)\right) - T_1\right] \quad (13)$$

Combining (9) (10) (12), it can be shown that,

$$V_L(k+1) - V_L(k) = \left(V(k+1) - V(k)\right)\left(V(k+1) + V(k)\right) = -c_L(2 - c_L)V^2(k) \quad (14)$$

Therefore, for $0 < c_L < 2$,the step difference of V_L would be negative semidefinite. Based on theorems in [4], now that we have a positive semidefinite Lyapunov function V_L in a time-invariant discrete system and $\Delta V_L \leq 0$, the equilibrium point is stable in the sense of Lyapunov if it is asymptotically stable for all the perturbed initial conditions $x_0 \in Z$, where Z is the largest invariant set in $\{x | V_L(x) = 0\}$. It is proved in [2] that $Z = \{T_{ivc} | \Delta V_L = 0\}$ in the vicinity of the desired operating point $\theta_{CA50}^{des} = 5°$, thus it follows that the feedback control law would converge to (15) when V_L is set to 0. Then a linear state equation is acquired by applying (15) to state (9), which cancels the nonlinear term.

$$x_r(k+1) = \left[-K_I\tau\left(\theta_{CA50}^{des} - \tilde{\theta}_{CA50}\left(m_f(k), T_{ivc}(k)\right)\right) + T_{ivc}(k) - T_1\right] / \left[0.9 f_c\left(T_{ivc}(k), m_f(k)\right) - T_1\right] \quad (15)$$

$$T_{ivc}(k+1) = \left(1 + K_I\tau g_1\left(m_f(k)\right)\right) T_{ivc}(k) + K_I\tau\left(g_0\left(m_f(k)\right) - \theta_{CA50}^{des}\right) \quad (16)$$

The state T_{ivc} is asymptotically stable if $\left|1 + K_I\tau g_1\left(m_f(k)\right)\right| < 1$, which can be achieved by choosing appropriate gain K_I. Note that the convergence of T_{ivc} would result in convergence of $q(k)$ because the tracking error is 0, which can be shown using (10) and (16). Thus the equilibrium at $\theta_{CA50}^{des} = 5°$ is stable in the sense of Lyapunov, which implies the desired combustion operating point would be reached using the controller described in (13).

4.2 Nonlinear Observer Design

The designed controller in (13) actually requires measurement of states at each step, of which $\theta_{CA50}(k)$ is available but $T_{ivc}(k)$ is not. Therefore, an observer is required to implement the feedback control law. The design of such observer relies on approximating $f_c\left(T_{ivc}(k), m_f(k)\right)$ as a quadratic polynomial

* Complete state equations, delay equations and algebraic equations for combustion are included in Appendix A.
Simulink Block diagram in Appendix B.
MATLAB code in Appendix C.

function of T_{ivc} at different fuel levels m_f, then it follows a rewritten version of the state equation in (9). Moreover, a similar quadratic approximation $\bar{\theta}_{CA50}$ is used for θ_{CA50} in (18), which converts the nonlinear term in (17) to a linear one.

$$T_{ivc}(k+1) = \left[l_0(m_f) + l_1(m_f)T_{ivc}(k) + l_2(m_f)T_{ivc}^2(k)\right]x_r(k+1) + T_1 \quad (17)$$
$$\bar{\theta}_{CA50} = h_0(m_f) + h_1(m_f)T_{ivc} + h_2(m_f)T_{ivc}^2 \quad (18)$$

Note that the different approximation for θ_{CA50} is used here to derive a linear state equation. Thus the resulting estimator would also possess a linear equation, resulting a linear error dynamics. The condition for exponential convergence of error to zero is then easy to find.

Define $\gamma_0 = l_0 - \frac{h_0 l_2}{h_2}, \gamma_1 = l_1 - \frac{h_1 l_2}{h_2}, \gamma_2 = \frac{l_2}{h_2}$, which are all functions of fueling level m_f only. Then combining (17) and (18), we obtain a linearized state equation in (19). The observer $\hat{T}_{ivc}$ is then designed as shown in (20) with an error dynamics $e(k) = T_{ivc}(k) - \hat{T}_{ivc}$ in (21).

$$T_{ivc}(k+1) = \gamma_1(m_f)x_r(k+1)T_{ivc}(k) + \gamma_2(m_f)x_r(k+1)\bar{\theta}_{CA50} + \gamma_0(m_f)x_r(k+1) + T_1 \quad (19)$$
$$\hat{T}_{ivc}(k+1) = \gamma_1(m_f)x_r(k+1)\hat{T}_{ivc}(k) + \gamma_2(m_f)x_r(k+1)\bar{\theta}_{CA50} + \gamma_0(m_f)x_r(k+1) + T_1 \quad (20)$$
$$e(k+1) = \gamma_1(m_f)x_r(k+1)e(k) \quad (21)$$

The error $e \to 0$ exponentially under the condition that $\left|\gamma_1(m_f)x_r(RBL)\right| < 1$ for all m_f and RBL profile, which is true for most of the cases. Thus the designed observer $\hat{T}_{ivc}$ is a zero-bias estimator of the state T_{ivc} when the state oscillation is small. Using the observer as the state measurement for (13), the feedback controller design is complete.

4.3 Robustness of Nonlinear Feedback Controller

In Section 4.1, we discussed local Lyapunov stability is guaranteed under the correct gain design $0 < c_L < 2$. However, to guarantee Lyapunov stability, the linear approximation in (11) must also hold, which means the system should be operated around the operating point. Considering the uncertainties in the model due to model mismatch or unknown disturbance, an estimate of the local region of attraction of the desired operating point would be very useful to examine the robustness of the proposed feedback control law.

The mathematical formulation of region of attraction estimation is detailed in Chiang's work [2]. To save space, we only highlight the key steps to rederive Chiang's approach to such estimation. First, the quadratic approximation in (18) is used to provide a more accurate approximation accounting for nonlinearity, which substitutes $\bar{\theta}_{CA50}$ for $\tilde{\theta}_{CA50}$ in (9) and (10) to form new state equations. Then the state equations are centered around the origin, transforming the closed-loop states to

$$x(k) = \left[\delta T_{\mathrm{ivc}}(k) \quad \delta q(k)\right]^T$$
$$A = \begin{bmatrix} 1 - c_L + K_I \tau g_1\left(m_f(k)\right) & -c_L K_I \\ \tau\sqrt{h_1^2\left(m_f(k)\right) - 4h_2\left(m_f(k)\right)\left(h_0\left(m_f(k)\right) - \theta_{CA50}^{\mathrm{des}}\right)} & 1 \end{bmatrix}$$
$$\Delta f\left(x(k)\right) = \left[0 \quad -\tau h_2\left(m_f(k)\right)\delta T_{\mathrm{ivc}}^2(k)\right]^T \quad , \quad (22)$$
$$x(k+1) = Ax(k) + \Delta f(x(k)), \quad (23)$$

Note that A is Hurwitz for all desired operating points at different fueling levels. Choose $V_A(k) = x^T(k)Px(k)$ as a Lyapunov function for the system (22). P is the solution to discrete-time Lyapunov equation $A^T PA - P + Q = 0$ with $Q = [1\,0; 0\,0]$ positive semi-definite. Determine the domain D around the origin where $\Delta V_A(k)$ is negative definite, and a constant $c > 0$, such that $\Omega_c = \{x | V_A(x) \le c\} \subset D$. Then the estimation of region of attraction would be the largest Ω_c we can find given the dynamics in (22) around the desired operating point.

* Complete state equations, delay equations and algebraic equations for combustion are included in Appendix A. Simulink Block diagram in Appendix B.
MATLAB code in Appendix C.

From the experiment results shown in [2], we could observe that when applying the observer based feedback control law to the full order system with manifold dynamics and extra thermodynamic relations in exhaust runner, θ_{CA50} achieves relatively good regulation with its mean value stabilized at desired value. When the fuel step changes, θ_{CA50} is regulated back to desired value in relatively short as well. Same regulation effect is observed even with nonlinearity uncertainty present. Therefore, the controller is rather robust with the observer.

4.4 Comparison with Other Control Strategies

In Chiang's work [2], a static feed-forward controller is also implemented using a fuel rate map developed with the full-order model in [1]. During small fuel steps, both controllers could regulate θ_{CA50}, but feedback controller has faster transient responses and much less overshoot, more smooth responses especially in temperature traces than the feedforward controller. During large fuel steps, the feedforward controller fails to regulate while feedback controller could still achieve regulation. This can be explained by i) the feedforward controller generates a step change in RBL command which results in large deviation in T_{ivc} ii) HCCI engine is sensitive to charge condition at IVC, such sudden changes would result in destabilizing of the combustion timing, which comes back causing more ill-conditioned IVC charge condition, causing the engine cycles to show unbounded behaviors. Therefore, the feedback controller is a better choice in terms of stabilizing the temperature at IVC during fuel step changes.

Apart from the controllers studied in [2], we think there could be other control strategies with better performance. Specifically, we think Model Predictive Control would be an interesting direction to look into. The HCCI engines are rather unstable, therefore, the stable charge conditions at IVC need to be guaranteed otherwise the engine could have bad combustion timing resulting in unwanted consequences. When the proposed stability condition fails, the feedback controller could result in unbounded behaviors. However, with MPC hard constraints can be imposed and will be satisfied, which should help with maintaining dynamics within a stable range around desired operating points. The drawback would be that nonlinear MPC requires much larger computational cost, which may cause delay for control decision.

5 Conclusion

The objective of our project was to reproduce the result of Chiang's work [2] by first building a HCCI engine model and implement feedback controller to control the combustion timing by stabilizing the temperature. Two models were built in Simulink following the literature, one was a full-order model and the other one was a simplified model focusing on temperature dynamics, but neither was completely calibrated to produce meaningful results. The main reasons for the unsuccessful model reproduction are (1) The initial condition we used for manifold dynamics may not be feasible (2) The parameters and their units in combustion model used might be different from the actual values used to produce results in literature. We generated results from a manifold dynamics test and combustion model test. The values of corresponding states are within reasonable ranges. Without further data support to identify suitable initial condition, it is difficult to further the results.

Though we don't have a working model to implement control on, we did look into and rederived the control strategies used in literature. The nonlinearity and unstable nature of HCCI engine actually gave us a good chance to learn about nonlinear control theory including controller design based on Lyapunov function and stability analysis. By comparing the feedforward and feedback controller, we learnt about excursive change in charge condition at IVC would result in unbounded behaviors of the engine and the importance of maintaining operating conditions near a desired point. We think MPC would help keeping charge conditions feasible and perhaps we could try to implement it if we remedy the model issue. Overall, we think HCCI engine control is a very interesting topic and the autoignition makes control design more difficult. We look forward to learning more about related research and perhaps working on it in the future.

* Complete state equations, delay equations and algebraic equations for combustion are included in Appendix A.
Simulink Block diagram in Appendix B.
MATLAB code in Appendix C.

6 References

[1] D.J. Rausen, A.G. Stefanopoulou, J.A. Kang, J.-M.And Eng, and T.-W Kuo. A mean-value model for control of homogeneous charge compression ignition (hcci) engines. *Transactions of the ASME. Journal of Dynamic Systems, Measurement and Control*, 3(3):355-362, September 2005. Appendix

[2] Chia-Jui Chiang, A. G. Stefanopoulou, and M. Jankovic. Nonlinear observer-based control of load transitions in homogeneous charge compression ignition engines. *IEEE Transactions on Control Systems Technology*, 15(3):438-448, May 2007. special issue in Control Applications in Automotive Engineering.

[3] Chia-Jui Chiang and A. G. Stefanopoulou. Stability analysis in homogeneous charge compression ignition (hcci) engines with high dilution. *IEEE Transactions on Control Systems Technology*, 15(2):209-219, March 2007

[4] J. Grizzle and J.-M. Kang, "Discrete-time control design with positive semi-definite lyapunov functions," *Syst. Control Lett.*, vol. 43, pp 287–292, 2001.

* Complete state equations, delay equations and algebraic equations for combustion are included in Appendix A.
Simulink Block diagram in Appendix B.
MATLAB code in Appendix C.

7 Appendix A (Equation)

7.1 Algebraic Equation for combustion

Equation in [1]:

$$b_{\text{bd}} = \frac{\text{AFR}_s + 1}{\text{AFR}_c + 1}(1 - b_c) + b_c$$

$$\frac{d}{dt}\text{AFR}_{\text{EGO}} = \frac{1}{\tau_{\text{EGO}}}(\text{AFR}_2 - \text{AFR}_{\text{EGO}})$$

$$\text{AFR}_2 = \frac{1 - b_2 + \text{AFR}_s}{b_2}.$$

$$\text{AR}(\theta_{\text{soc}}) = 1 \text{ where } \text{AR}(\theta) = \int_{\theta_{\text{ivc}}}^{\theta} RR(\vartheta)d\vartheta$$

$$\text{RR}(\vartheta) = Ap_{\text{ivc}}^{n} v_{\text{ivc}}^{n_c n}(\vartheta)\exp\left(-\frac{E_a v_{\text{ivc}}^{1-n_c}(\vartheta)}{RT_{\text{ivc}}}\right)$$

$$\theta_c = \theta_{\text{soc}} + \Delta\theta$$

$$\text{where } \Delta\theta = k(T_{\text{soc}})^{(-2/3)}(T_m)^{1/3}\exp\left(\frac{E_c}{3R_u T_m}\right)$$

$$\text{and } T_m = T_{\text{soc}} + e(1 - b_c)\Delta T$$

$$\Delta T = \frac{Q_{\text{LHV}}}{c_v(1 + AFR_c)}$$

$$e = a_0 + a_1 k$$

$$k = b_{k0} + b_{k1}\theta_{\text{soc}} + b_{k2}\theta_{\text{soc}}^2$$

$$T_{ac} = T_{bc} + (1 - b_c)\Delta T \text{ and } p_{ac} = p_{bc}T_{ac}/T_{bc}$$

$$T_{\text{bd}} = T_{\text{evo}}\frac{p_2}{p_{\text{evo}}}^{(n_e-1)/n_e} + \Delta T_{\text{bd}}$$

Equation in [2]:

$$\int_{\theta_{\text{ivc}}}^{\theta_{\text{soc}}} Ap_{\text{ivc}}^{n} v_{\text{ivc}}^{n_c n}(\vartheta)\exp\left(-\frac{E_a v_{\text{ivc}}^{1-n_c}(\vartheta)}{RT_{\text{ivc}}}\right)d\vartheta = 1$$

where

$$v_x(\vartheta_y) = V_c(\vartheta_x)/V_c(\vartheta_y)$$
$$\theta_{\text{soc}} = \theta_{CA01}$$
$$T_{\text{soc}} = T_{\text{ivc}} v_{\text{ivc}}^{(n_c-1)}(\theta_{\text{soc}})$$
$$\Delta\theta = k(T_{\text{soc}})^{(-2/3)}(T_m)^{1/3}\exp\left(\frac{E_c}{3R_u T_m}\right)$$

where

$$T_m = T_{\text{soc}} + e\Delta T$$
$$\Delta T = \frac{Q_{\text{LHV}} m_f}{C_v m_c}$$
$$e = b_0 + b_1\theta_{\text{soc}} + b_2\theta_{\text{soc}}^2$$

$$\theta_{CA50} = \theta_{\text{soc}} + .55\Delta\theta$$
$$\theta_c = \theta_{CA90} = \theta_{\text{soc}} + \Delta\theta$$
$$T_{bc} = T_{\text{ivc}} v_{\text{ivc}}^{(n_c-1)}(\theta_c)$$
$$p_{bc} = p_{\text{ivc}} v_{\text{ivc}}^{n_c}(\theta_c)$$
$$T_{ac} = T_{bc} + \Delta T$$
$$p_{ac} = p_{bc}T_{ac}/T_{bc}$$
$$T_{\text{evo}} = T_{ac} v_c^{(n_e-1)}(\theta_{\text{evo}})$$
$$p_{\text{evo}} = p_{ac} v_c^{n_e}(\theta_{\text{evo}})$$
$$T_{\text{bd}} = T_{\text{evo}}(p_2/p_{\text{evo}})^{(n_e-1)/n_e}$$

* Complete state equations, delay equations and algebraic equations for combustion are included in Appendix A.
Simulink Block diagram in Appendix B.
MATLAB code in Appendix C.

7.2 State Equation for [2]

$$
\begin{aligned}
\frac{d}{dt}p_1 &= \frac{RT_1}{V_1}(W_{01} - W_{1c}) \\
\frac{d}{dt}m_2 &= W_{c2} - W_{20} - W_{2c} \\
\frac{d}{dt}b_2 &= \frac{W_{c2}(b_{\mathrm{er}} - b_2)}{m_2} \\
\frac{d}{dt}p_2 &= \frac{\gamma R}{V_2}\left(W_{c2}T_{\mathrm{er}} - (W_{20} + W_{2c})T_2\right) \\
&\quad - \frac{(\gamma - 1)A_2 h_2}{V_2}(T_2 - T_w) \\
W_{c2}(t+\tau) &= W_{1c}(t) + W_f(t) + W_{2c}(t) \\
b_{\mathrm{er}}(t+\tau) &= b_{\mathrm{bd}}(t) \quad \text{where } \tau = N/120 \\
T_{\mathrm{er}}(t+\tau) &= \frac{T_w T_{\mathrm{bd}}(t)}{(1-\alpha_{ht})T_{\mathrm{bd}}(t) + \alpha_{ht}T_w}
\end{aligned}
$$

where

$$\alpha_{ht} = \exp\left(\frac{-4h_{\mathrm{er}}RT_w}{C_p D_{\mathrm{er}} p_2}t_r\right)$$

$$\frac{d}{dt}T_{\mathrm{er}} = -\frac{A_{\mathrm{er}}h_{\mathrm{er}}}{C_p m_{\mathrm{er}}}(T_{\mathrm{er}} - T_w),\ T_{\mathrm{er}}(0) = T_{\mathrm{bd}}(t-\tau)$$

with

$$m_{\mathrm{er}} = \frac{p_2 V_{\mathrm{er}}}{RT_{\mathrm{er}}}$$

and

$$A_{\mathrm{er}} = 4V_{\mathrm{er}}/D_{\mathrm{er}}.$$

* Complete state equations, delay equations and algebraic equations for combustion are included in Appendix A.
Simulink Block diagram in Appendix B.
MATLAB code in Appendix C.

Appendix B Simulink Block Diagrams

B.1 Full-order Model from Rausen's Work [1]

Full Model:

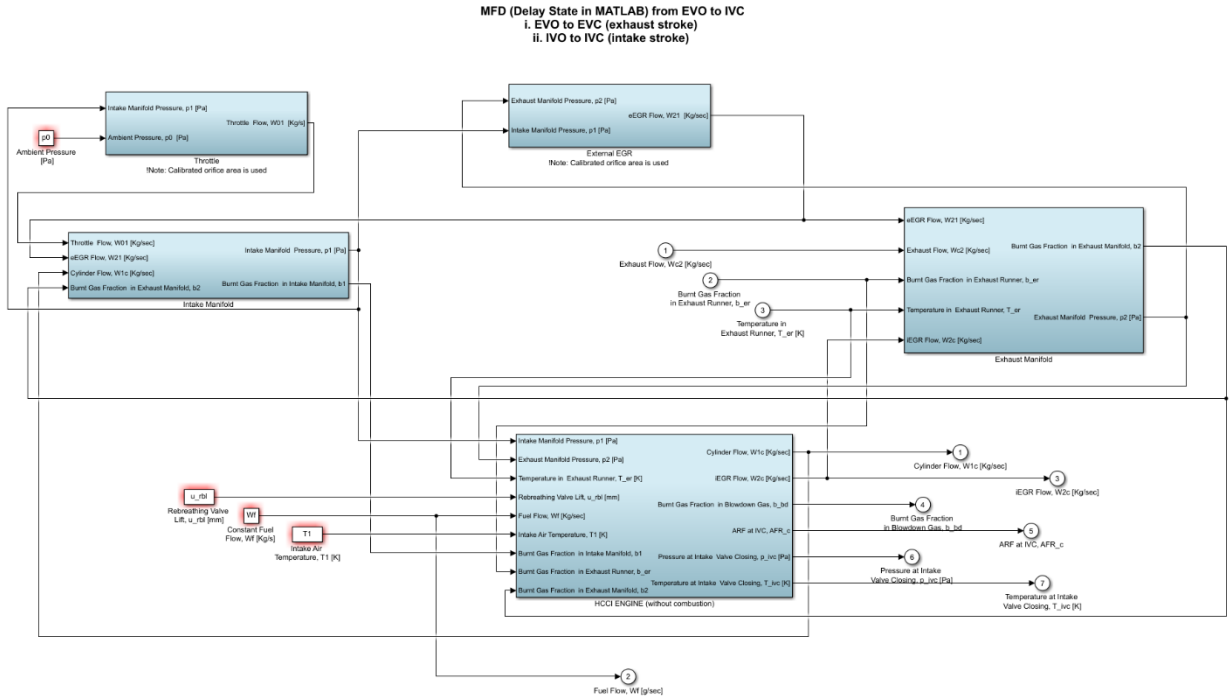

Throttle:

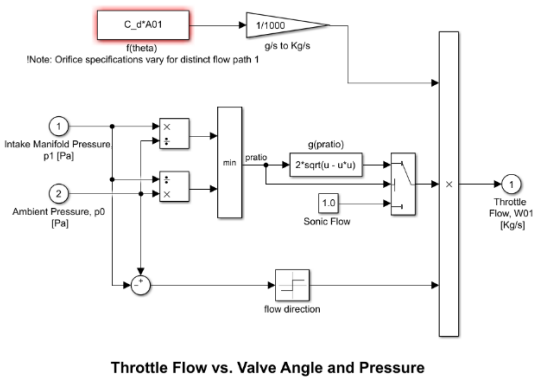

Intake Manifold:

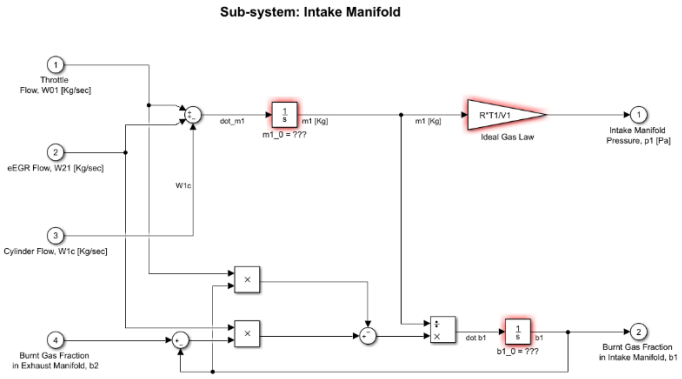

External EGR:

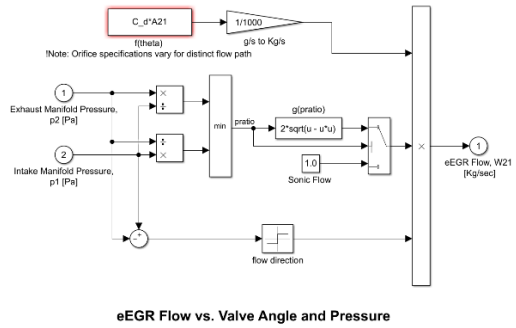

Exhaust Manifold:

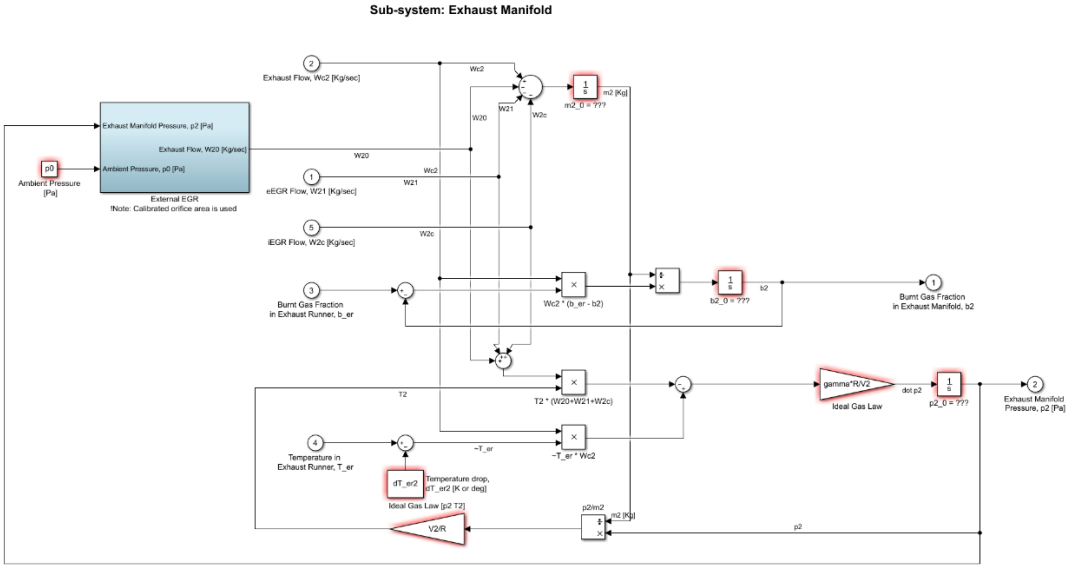

Combustion Setup:

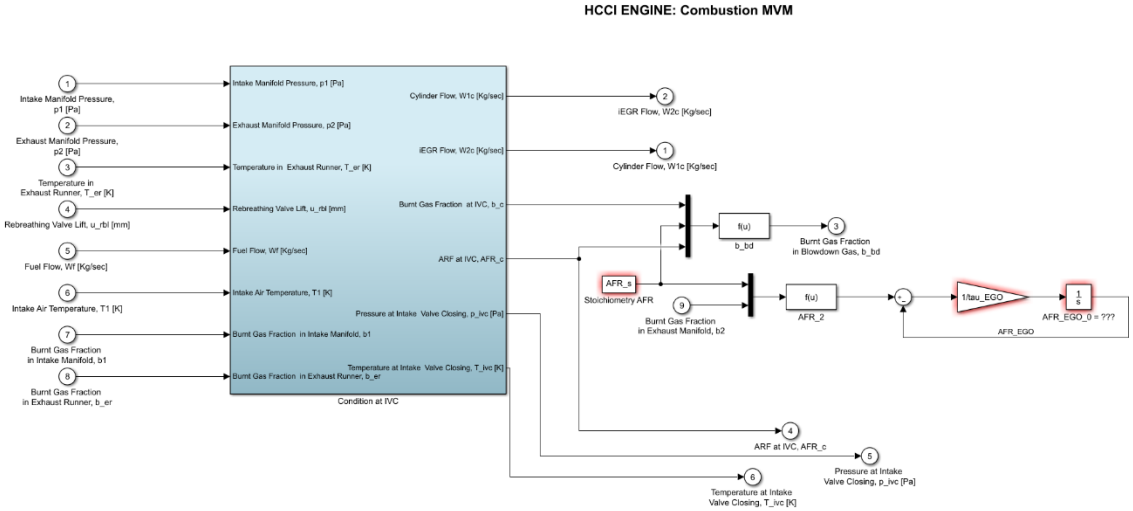

Conditions at Intake Valve Closing:

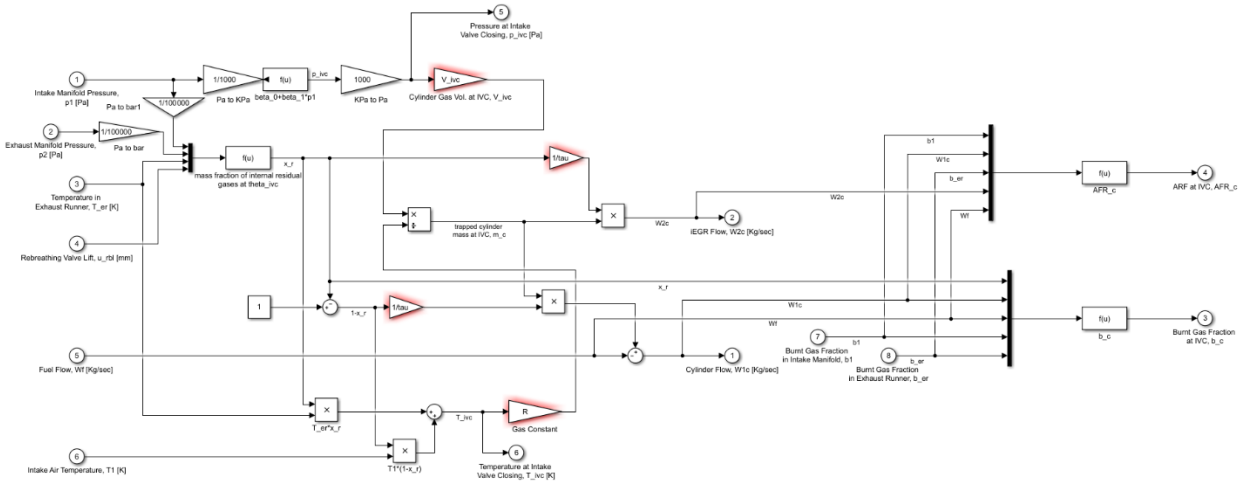

B.2 Simplified Model in Chiang's Work [2]

Full Model:

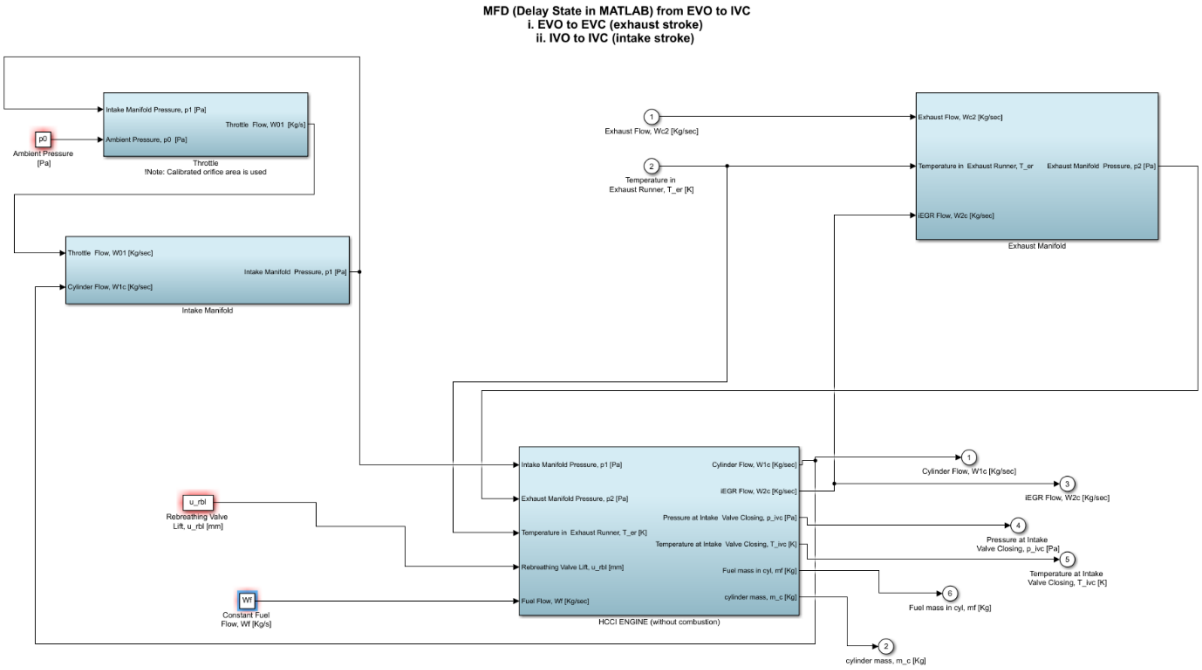

Throttle:

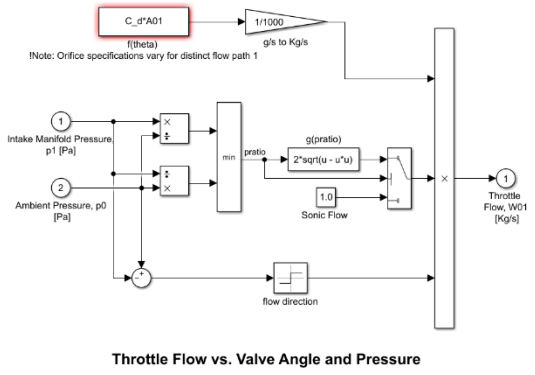

Throttle Flow vs. Valve Angle and Pressure

Intake Manifold:

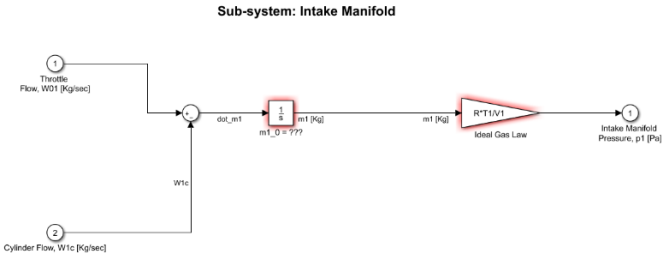

Exhaust Manifold:

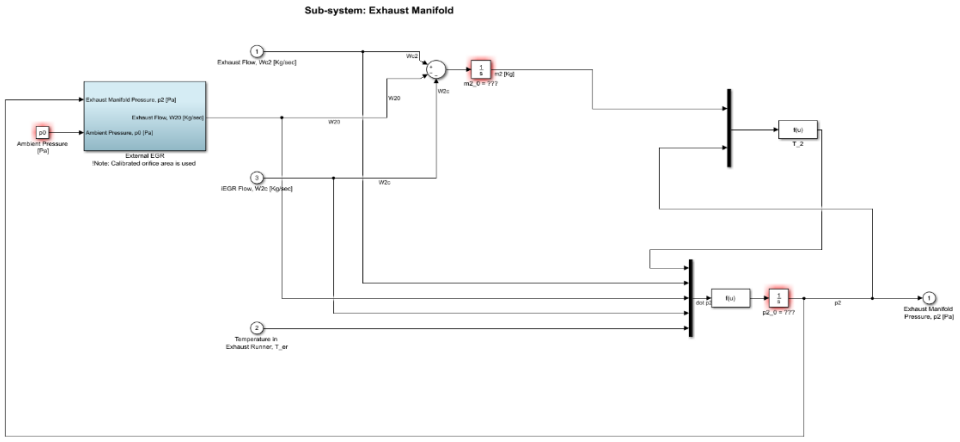

Conditions at Intake Valve Closing:

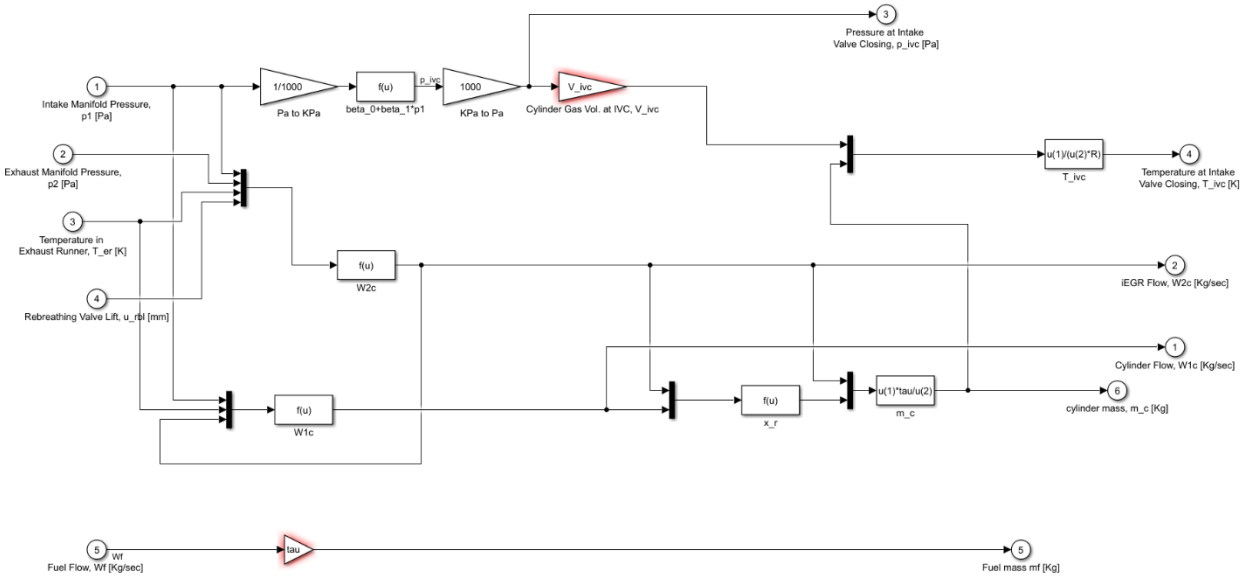

Appendix. C MATLAB code

C1. Full-order Model Simulation Script

Simulation script:

```
close all; clc;
clear all;
%% HCCI Eng. Model parameters
load_param;
%% Initial Condition (States)
m1_0        = p0*V1/(R*T1); % Intake manifold charge mass, Kg
m2_0        = p0*V2/(R*T1); % Exhaust manifold charge mass, Kg
b1_0        = 0.5; % Intake manifold burnt gas fraction
b2_0        = 1; % Exhaust manifold burnt gas fraction
p2_0        = p0; % Exhaust manifold pressure, KPa
AFR_EGO_0   = AFR_s; % AFR at EGO sensor
%% First engine cycle
%% MFD EVO to IVC
t_end       = tau / 2;
tstep       = 0.001;

time_in     = transpose(0:tstep:t_end);
Wc2_in      = 0.1*ones(size(time_in,1),1);
b_er_in     = 0.7*ones(size(time_in,1),1);
T_er_in     = 550*ones(size(time_in,1),1);

UT_in       = [time_in Wc2_in b_er_in T_er_in];
%% Simulation
options     = simset;
[time,states,output] = sim('hcci_eng',[0 t_end],options,UT_in);
% Index  1      2       3       4       5       6           7
% States [m1_0  p2_0    b1_0    m2_0    b2_0    AFR_EGO_0]
% Output [W1c   Wf      W2c     b_bd    AFR_c   p_ivc       T_ivc]

[CA50, T_bd] = HCCI_Combustion(output(end,5), output(end,6), output(end,7), states(end,2));



%% More engine cycles
cycle_num   = 10;
data_50 = zeros(cycle_num+1, 1);
data_50(1) = CA50;
for i = 1:cycle_num
    %% Initial State Update
    m1_0        = states(end,1); % Intake manifold charge mass, Kg
    m2_0        = states(end,4); % Exhaust manifold charge mass, Kg
    b1_0        = states(end,3); % Intake manifold burnt gas fraction
    b2_0        = states(end,5); % Exhaust manifold burnt gas fraction
    p2_0        = states(end,2); % Exhaust manifold pressure, KPa
    AFR_EGO_0   = states(end,6); % AFR at EGO sensor
    %% Delay States
    t_end       = tau;
    tstep       = 0.001;
    Wc2_in      = (sum(output(end,1:3)))*ones(size(time_in,1),1);
    b_er_in     = output(end,4)*ones(size(time_in,1),1);
    T_er_in     = T_bd*ones(size(time_in,1),1);
    %% Simulation
    UT_in       = [time_in Wc2_in b_er_in T_er_in];
    options     = simset;
    [time,states,output] = sim('hcci_eng',[0 t_end],options,UT_in);
    %% Combustion
    [CA50, T_bd] = HCCI_Combustion(output(end,5), output(end,6), output(end,7), ...
        states(end,2));
    data_50(i+1) = CA50;

end
```

Load Parameter Script:

```
%% Orifice specification A01 A20 A21 are unknow for now...
C_d     = 1; % Contraction coefficient (assume)
f       = @(u) 2.821 - 0.05231*u + 0.10299*u*u - 0.00063*u*u*u;
A01     = f(90); % Calibrated throttle orifice
A20     = f(70); % Calibrated exhaust orifice
A21     = f(50); % Calibrated eEGR valve orifice

%% Default Running Condition;
N       = 1000; % Fixed engine speed, rpm
Wf      = 11.9e-6; % Constant fuel injection rate, Kg/sec
AFR_s   = 20; % Stoichiometry AFR (run lean)
u_rbl   = 2; % Rebreathing valve lift, mm
tau     = 120 / N; % Engine cycle delay, sec
tau_EGO = 0.08; % EGO sensor time constant, sec; from HW4

p0          = 101000; % ambient pressure, Pa
T1          = 90 + 273.15; % intake air temperature, K
dT_er2      = 75; % temperature drop based on test data from the exhaust runner to exhaust ...
    manifold

V1          = 0.0013; % Intake manifold volume, m^3 !REFChiangIEEE
V2          = 0.015; % Exhaust manifold volume, m^3 !REFChiangIEEE
V_d         = 5.5e-4; % Stroke (displacement) Volume, m^3
CR          = 14; % Cylinder compression ratio
V_TDC       = V_d / (CR - 1); % V_c when piston at TDC, m^3
V_ivc       = V_d + V_TDC; % Cylinder Volume of Intake Valve Closing (DBC), m^3

gamma       = 1.4; % ratio of specific heats for air (assume does not depend on inert gas ...
    fraction ACC04.P3)
%% Params in Appendix Table
alpha_1     = 0.752; % Modulation of x_r by u_bbl
alpha_2     = -0.180; % Modulation of x_r by u^2_bbl
alpha_3     = 0.015; % Modulation of x_r by u^3_bbl

beta_0      = 1.035; % Constant term of p_ivc, KPa
beta_1      = 1.1568; % Linear term of p_ivc

% dT_bd       = -65; % Blowdown temperature difference

kappa_0     = -2.2107; % Constant term of x_r
kappa_1     = 61.5556; % Linear term of x_r
kappa_2     = 4.6052; % p_2 exponent in x_r
kappa_3     = 0.964; % p_1 exponent in x_r

% a0          = 1.0327; % Constant term in e parametrization
% a1          = -5.45; % Linear term, e dependence on k
%
% A           = 2500; % Arrhenius scaling constant
%
% bk0         = 0.162; % const term in k parametrization
% bk1         = 0.005; % Linear term in k dependence on theta_soc
% bk2         = 0.001; % Square term in k dependence on theta_soc
%
% Ea          = 6317; % Arrhenius activation energy
% Ec          = 185; % Activation energy, kJ/mol

nbd         = 1.35; % Adiabatic blowdown coefficient
nc          = 1.30; % Polytropic constant during compression
ne          = 1.35; % Polytropic constant during expansion

R           = 296.25; % gas constant, J/KgK
Ru          = 8.314; % Universal gas constant, J/mol K
```

Combustion Script:

```
function [CA50, T_bd] = HCCI_Combustion(AFR_c, p_ivc, T_ivc, p_2)
%% Params for Arrhenius Integral & Combustion
%% Arrhenius Intergral Params
A           = 0.04167; % Arrhenius scaling constant
n           = 1.367; % reaction  s sensitivity to pressure REF2[10]
Ea          = 6317; % Arrhenius activation energy
R           = 296.25; % gas constant, J/KgK
%% Combustion Duration Params
b0          = 0.4086; % const term in k parametrization
b1          = -0.0839; % Linear term in k dependence on theta_soc
b2          = -0.0153; % Square term in k dependence on theta_soc

k           = 0.5397;

c_v         = 1.4; % constant volume specific heat (KJ/Kg.K) [17]
Q_LHV       = 43960; % low heating value of the fuel (KJ/Kg)

Ec          = 185; % Activation energy, kJ/mol
Ru          = 8.314; % Universal gas constant, J/mol K
nc          = 1.30; % Polytropic constant during compression
ne          = 1.35; % Polytropic constant during expansion

dT_bd       = -65; % Blowdown temperature difference
%% Load params for cylinder
V_d         = 5.5e-4; % Stroke (displacement) Volume, m^3
CR          = 14; % Cylinder compression ratio
V_TDC       = V_d / (CR - 1); % Vc when piston at TDC, m^3
%% Params for cylinder (Calculated)
B           = 8.6e-2; % Bore Diameter, m
r           = 2*V_d/(pi*B^2); % Crankshaft radius, m
rod_ratio   = 1.54; % GM L61 Ecotec Engine (2.2L);
l           = rod_ratio*2*r; % Connecting rod length
%% Solve theta_soc
syms theta T;
s           = r*(1-cos(theta)+l/r*(1-sqrt(1-(r*sin(theta)/l)^2))); % stroke, m
Vc          = V_TDC + s*pi*B^2/4;

theta_ivc   = 180*pi/180; % Crank angle at IVC, rad (Fig. 5)
theta_evo   = 180*pi/180; % Crank angle at EVO, rad (Fig. 5)
V_ivc       = double(subs(Vc, theta, theta_ivc));% Cylinder Volume of Intake Valve Closing ...
    (DBC), m^3

%% Phase 1: IVC to SOC
RR_theta    = A*((p_ivc*1e-5)^n)*(V_ivc/Vc)^(nc*n)*exp(-(Ea*(V_ivc/Vc)^(1-nc))/(R*T_ivc));

threshold   = 0.01;
step_len    = 0.001;
T_tmp       = -theta_ivc:step_len:0;
T           = abs(T_tmp);
Riemann_sum = 0;
theta_soc   = 0;
for i = 1:size(T,2)
    % v = double(subs(V_ivc/Vc, theta, T(i)))
    Riemann_sum = Riemann_sum + step_len * double(subs(RR_theta, theta, T(i)));
    %disp(Riemann_sum);
    if abs(Riemann_sum - 1) <= threshold
        theta_soc = T(i);
        break
    end
end
v_soc       = double(subs(V_ivc/Vc, theta, theta_soc));
T_soc       = T_ivc*v_soc^(nc-1);
% [theta_soc, T_soc] = AR_solver(p_ivc, T_ivc);
%% Phase 2: Combustion Duration
e           = b0 + b1*theta_soc + b2*theta_soc^2; % Verified Model from ChiangIEEE
```

```
Delta_T     = Q_LHV/c_v/(1+AFR_c);
Tm          = T_soc + e*Delta_T; % Verified effective mean T Model from ChiangIEEE
Delta_theta = k*T_soc^(-2/3)*Tm^(1/3)*exp(Ec/(3*Ru*Tm));

theta_c     = theta_soc + Delta_theta;
CA50        = theta_soc + 0.55*Delta_theta;
% [theta_c, Delta_T, CA50, Tm] = comb_dur(b_c, AFR_c, theta_soc, T_soc);
%% Phase 3: Instantanous Heat Release
%% Params Before Combustion
T_bc        = T_ivc*double(subs(V_ivc/Vc, theta, theta_c))^(nc-1);
p_bc        = p_ivc*double(subs(V_ivc/Vc, theta, theta_c))^nc;
%% Params After Combustion
T_ac        = T_bc + Delta_T+100; % Verified Model from ChiangIEEE
p_ac        = p_bc*T_ac/T_bc;
% [T_ac, p_ac] = heat_release(b_c, theta_c, Delta_T, p_ivc, T_ivc);
%% Phase 4: Polytropic Expansion
V_c          = double(subs(Vc, theta, theta_c)); % Cylinder Volume at theta_c, m^3
T_evo        = T_ac*double(subs(V_c/Vc, theta, theta_evo))^(ne-1);
p_evo        = p_ac*double(subs(V_c/Vc, theta, theta_evo))^ne;
% [T_evo, p_evo] = poly_exp(T_ac, p_ac, theta_c);
%% Phase 5: Exhaust Blowdown
T_bd         = T_evo*(p_2/p_evo)^((ne-1)/ne) + dT_bd;
%% Output and Graph
plot([-theta_ivc -theta_soc theta_c theta_c theta_evo theta_evo]*180/pi, [T_ivc T_soc Tm ...
    T_ac T_evo T_bd],'o');
end
```

C2. Simplified Model Simulation Script: Simulation script:

```
close all; clc;
clear all;
%% HCCI Eng. Model parameters
load_param;
%% Initial Condition (States)
m1_0        = p0*V1/(R*T1); % Intake manifold charge mass, Kg
m2_0        = p0*V2/(R*T1); % Exhaust manifold charge mass, Kg
p2_0        = p0; % Exhaust manifold pressure, KPa
%% First engine cycle
%% MFD EVO to IVC
t_end       = tau/4;
tstep       = 0.001;

time_in     = transpose(0:tstep:t_end);
Wc2_in      = -0.001*ones(size(time_in,1),1);
T_er_in     = 450*ones(size(time_in,1),1);

UT_in       = [time_in Wc2_in T_er_in];
%% Simulation
options     = simset;
[time,states,output] = sim('hcci_eng',[0 t_end],options,UT_in);
% Index  1      2       3       4       5       6           7
% States [m1_0  p2_0    m2_0]
% Output [W1c   m_c     W2c     p_ivc   T_ivc   m_f]

[CA50, T_bd] = HCCI_Combustion(output(end,6), output(end,2), output(end,4), output(end,5), ...
    states(end,2));



%% More engine cycles
cycle_num   = 10;
data_50 = zeros(cycle_num+1, 1);
data_50(1) = CA50;
for i = 1:cycle_num
    %% Initial State Update
    m1_0        = states(end,1); % Intake manifold charge mass, Kg
    m2_0        = states(end,4); % Exhaust manifold charge mass, Kg
    b1_0        = states(end,3); % Intake manifold burnt gas fraction
    b2_0        = states(end,5); % Exhaust manifold burnt gas fraction
    p2_0        = states(end,2); % Exhaust manifold pressure, KPa
    AFR_EGO_0   = states(end,6); % AFR at EGO sensor
    %% Delay States
    t_end       = tau;
    tstep       = 0.001;
    Wc2_in      = (sum(output(end,1:3)))*ones(size(time_in,1),1);
    b_er_in     = output(end,4)*ones(size(time_in,1),1);
    T_er_in     = T_bd*ones(size(time_in,1),1);
    %% Simulation
    UT_in       = [time_in Wc2_in b_er_in T_er_in];
    options     = simset;
    [time,states,output] = sim('hcci_eng',[0 t_end],options,UT_in);
    %% Combustion
    [CA50, T_bd] = HCCI_Combustion(output(end,5), output(end,6), output(end,7), ...
        states(end,2));
    data_50(i+1) = CA50;

end
```

Load Parameter Script:

```
%% Orifice specification A01 A20 A21 are unknow for now...
C_d     = 1; % Contraction coefficient (assume)
f       = @(u) 2.821 - 0.05231*u + 0.10299*u*u - 0.00063*u*u*u;
```

```
A01     = f(90); % Calibrated throttle orifice
A20     = f(70); % Calibrated exhaust orifice
A21     = f(50); % Calibrated eEGR valve orifice

%% Default Running Condition;
N       = 1000; % Fixed engine speed, rpm
Wf      = 11.9e-6; % Constant fuel injection rate, Kg/sec
AFR_s   = 20; % Stoichiometry AFR (run lean)
u_rbl   = 3; % Rebreathing valve lift, mm
tau     = 120 / N; % Engine cycle delay, sec
tau_EGO = 0.08; % EGO sensor time constant, sec; from HW4

p0          = 101000; % ambient pressure, Pa
T1          = 90 + 273.15; % intake air temperature, K
dT_er2      = 75; % temperature drop based on test data from the exhaust runner to exhaust ...
    manifold

V1          = 0.0013; % Intake manifold volume, m^3 !REFChiangIEEE
V2          = 0.015; % Exhaust manifold volume, m^3 !REFChiangIEEE
A2          = 0.3149; % Exh manifold heat transfer area m^2
h2          = 267; % Exh manifold heat transfer coeff W/m^2-K
T_w         = 400; %wall temperature K
V_d         = 5.5e-4; % Stroke (displacement) Volume, m^3
CR          = 14; % Cylinder compression ratio
V_TDC       = V_d / (CR - 1); % V_c when piston at TDC, m^3
V_ivc       = V_d + V_TDC; % Cylinder Volume of Intake Valve Closing (DBC), m^3
V_BDC       = V_ivc;

gamma       = 1.4; % ratio of specific heats for air (assume does not depend on inert gas ...
    fraction ACC04.P3)
%% Params in Appendix Table
alpha       = 0.5794;

beta_0      = 1.035; % Constant term of p_ivc, KPa
beta_1      = 1.1568; % Linear term of p_ivc

% dT_bd       = -65; % Blowdown temperature difference

kappa_0     = 0.5729; % Constant term of x_r
kappa_1     = -0.52039; % Linear term of x_r

% a0          = 1.0327; % Constant term in e parametrization
% a1          = -5.45; % Linear term, e dependence on k
%
% A           = 2500; % Arrhenius scaling constant
%
% bk0         = 0.162; % const term in k parametrization
% bk1         = 0.005; % Linear term in k dependence on theta_soc
% bk2         = 0.001; % Square term in k dependence on theta_soc
%
% Ea          = 6317; % Arrhenius activation energy
% Ec          = 185; % Activation energy, kJ/mol

nbd         = 1.35; % Adiabatic blowdown coefficient
nc          = 1.30; % Polytropic constant during compression
ne          = 1.35; % Polytropic constant during expansion

R           = 296.25; % gas constant, J/KgK
Ru          = 8.314; % Universal gas constant, J/mol K
```

Combustion Script:

```
function [CA50, T_bd] = HCCI_Combustion(m_f, m_c, p_ivc, T_ivc, p_2)
%% Params for Arrhenius Integral & Combustion
%% Arrhenius Intergral Params
A           = 0.4167; % Arrhenius scaling constant
n           = 1.367; % reaction  s sensitivity to pressure REF2[10]
Ea          = 1831930; % Arrhenius activation energy
R           = 296.25; % gas constant, J/KgK
%% Combustion Duration Params
b0          = 0.4086; % const term in k parametrization
b1          = -0.0839; % Linear term in k dependence on theta_soc
b2          = -0.0153; % Square term in k dependence on theta_soc

k           = 0.5397;

c_v         = 0.740625; % constant volume specific heat (J/Kg.K) [17]
Q_LHV       = 44000; % low heating value of the fuel (KJ/Kg)

Ec          = 185; % Activation energy, KJ/mol
Ru          = 8.314; % Universal gas constant, J/mol K
nc          = 1.30; % Polytropic constant during compression
ne          = 1.35; % Polytropic constant during expansion

%% Load params for cylinder
V_d         = 5.5e-4; % Stroke (displacement) Volume, m^3
CR          = 14; % Cylinder compression ratio
V_TDC       = V_d / (CR - 1); % Vc when piston at TDC, m^3
%% Params for cylinder (Calculated)
B           = 8.6e-2; % Bore Diameter, m
r           = 2*V_d/(pi*B^2); % Crankshaft radius, m
rod_ratio   = 1.54; % GM L61 Ecotec Engine (2.2L);
l           = rod_ratio*2*r; % Connecting rod length
%% Solve theta_soc
syms theta T;
s           = r*(1-cos(theta)+l/r*(1-sqrt(1-(r*sin(theta)/l)^2))); % stroke, m
Vc          = V_TDC + s*pi*B^2/4;

theta_ivc   = 180*pi/180; % Crank angle at IVC, rad (Fig. 5)
theta_evo   = 180*pi/180; % Crank angle at EVO, rad (Fig. 5)
V_ivc       = double(subs(Vc, theta, theta_ivc));% Cylinder Volume of Intake Valve Closing ...
    (DBC), m^3

%% Phase 1: IVC to SOC
RR_theta    = A*((p_ivc*1e-3)^n)*(V_ivc/Vc)^(nc*n)*exp(-(Ea*(V_ivc/Vc)^(1-nc))/(R*T_ivc));
% p_ivc in KPa
threshold   = 0.01;
step_len    = 0.001;
T_tmp       = -theta_ivc:step_len:0;
T           = abs(T_tmp);
Riemann_sum = 0;
% theta_soc   = 0;
for i = 1:size(T,2)
    % v = double(subs(V_ivc/Vc, theta, T(i)))
    Riemann_sum = Riemann_sum + step_len * double(subs(RR_theta, theta, T(i)));
    % disp(Riemann_sum);
    if abs(Riemann_sum - 1) <= threshold
        theta_soc = T(i);
        break
    end
end
v_soc       = double(subs(V_ivc/Vc, theta, theta_soc));
T_soc       = T_ivc*v_soc^(nc-1);
% [theta_soc, T_soc] = AR_solver(p_ivc, T_ivc);
%% Phase 2: Combustion Duration
e           = b0 + b1*theta_soc + b2*theta_soc^2; % Verified Model from ChiangIEEE
Delta_T     = Q_LHV*m_f/c_v/m_c;
```

```
Tm          = T_soc + e*Delta_T; % Verified effective mean T Model from ChiangIEEE
Delta_theta = k*T_soc^(-2/3)*Tm^(1/3)*exp(Ec/(3*Ru*Tm));

theta_c     = theta_soc + Delta_theta;
CA50        = theta_soc + 0.55*Delta_theta;
% [theta_c, Delta_T, CA50, Tm] = comb_dur(b_c, AFR_c, theta_soc, T_soc);
%% Phase 3: Instantanous Heat Release
%% Params Before Combustion
T_bc        = T_ivc*double(subs(V_ivc/Vc, theta, theta_c))^(nc-1);
p_bc        = p_ivc*double(subs(V_ivc/Vc, theta, theta_c))^nc;
%% Params After Combustion
T_ac        = T_bc + Delta_T; % Verified Model from ChiangIEEE
p_ac        = p_bc*T_ac/T_bc;
% [T_ac, p_ac] = heat_release(b_c, theta_c, Delta_T, p_ivc, T_ivc);
%% Phase 4: Polytropic Expansion
V_c          = double(subs(Vc, theta, theta_c)); % Cylinder Volume at theta_c, m^3
T_evo        = T_ac*double(subs(V_c/Vc, theta, theta_evo))^(ne-1);
p_evo        = p_ac*double(subs(V_c/Vc, theta, theta_evo))^ne;
% [T_evo, p_evo] = poly_exp(T_ac, p_ac, theta_c);
%% Phase 5: Exhaust Blowdown
T_bd         = T_evo*(p_2/p_evo)^((ne-1)/ne);
%% Output and Graph
plot([-theta_ivc -theta_soc theta_c theta_c theta_evo theta_evo]*180/pi, [T_ivc T_soc Tm ...
    T_ac T_evo T_bd],'o-');
end
```